Distinct Molecular Recognition of Calmodulin-Binding Sites in the Neuronal and Macrophage Nitric Oxide Synthases: A Surface Plasmon Resonance Study†

Martin Zoche,‡ Michael Bienert,§ Michael Beyermann,§ and Karl-Wilhelm Koch*,‡

Institut für Biologische Informationsverarbeitung, Forschungszentrum Jülich, Postfach 1913, D-52425 Jülich, Germany, and Forschungsinstitut für Molekulare Pharmakologie, Alfred-Kowalke-Strasse 4, D-10315 Berlin, Germany

Received February 23, 1996; Revised Manuscript Received May 2, 1996⊗

ABSTRACT: The neuronal nitric oxide synthase and the macrophage nitric oxide synthase are differently regulated by Ca^{2+}/calmodulin. We investigated the dynamics of calmodulin binding to the putative calmodulin-binding sites in both nitric oxide synthases. Peptides derived from the putative calmodulin-binding sites were synthesized and immobilized to a dextran layer of a biosensor chip. Complex formation of calmodulin and the peptides was monitored by surface plasmon resonance spectroscopy and recorded as sensorgrams. We determined a dissociation constant K_D of 5.0×10^{-9} M for the neuronal nitric oxide synthase and calmodulin. The association rate constant and the dissociation rate constant were $k_a = 1.58 \times 10^5$ M^{-1} s^{-1} and $k_d = 7.87 \times 10^{-4}$ s^{-1}, respectively. Sensorgrams obtained with the macrophage nitric oxide synthase peptide were remarkably different. Calmodulin, once bound to the peptide, did not dissociate. Association of calmodulin to the peptide occurred with the same rate constants ($k_a = 3 \times 10^4$ M^{-1} s^{-1}) regardless of the presence or absence of Ca^{2+}. The affinity was in the subnanomolar range ($K_D < 0.1 \times 10^{-9}$ M). We conclude that the extremely tight binding of calmodulin to the NOS-II is solely controlled by the calmodulin-binding segment and not by other parts of the protein.

The gas molecule nitric oxide (NO)[1] is involved as a messenger in many biological processes, including for example blood flow, neuromodulation, secretion, and inflammation (Bredt & Snyder, 1994; Schmidt & Walter, 1994; Marletta, 1994; Nathan & Xie, 1994; Griffith & Stuehr, 1995). NO is synthesized by the enzyme nitric oxide synthase (NOS) which converts L-arginine to L-citrulline. Three isoforms of NOS have been isolated, cloned, and functionally characterized (Bredt et al., 1991; Jannssens et al., 1992; Lamas et al., 1992; Xie et al., 1992; Lyons et al., 1992; Lowenstein et al., 1992). The forms NOS-I and NOS-III, first identified in neurons and endothelial cells, are activated at increased Ca^{2+} concentrations ([Ca^{2+}]) via Ca^{2+}/calmodulin (CaM). Another form (NOS-II) is mainly present in macrophages and independent of Ca^{2+}; however, it is tightly bound to CaM (Cho et al., 1992). The amino acid sequences of all three isoforms contain a putative CaM-binding motif that is present in Ca^{2+}/CaM-regulated enzymes and crucial for target recognition by CaM (O'Neil & DeGrado, 1990; James et al., 1995; Crivici & Ikura, 1995). The CaM-binding domain is located near the center of the enzyme separating the C-terminal reductase and the N-terminal oxygenase domain. During catalysis, electrons flow from NADPH in the oxygenase domain to the heme group in the reductase domain, when CaM is bound to its binding site (Abou-Soud & Stuehr, 1993). Electron flow studies also indicated that binding of CaM induces a conformational change that correctly aligns the two domains for interdomain electron transfer. However, depending on the electron acceptor, electron flow does not necessarily require Ca^{2+}/CaM (Schmidt et al., 1992). It was hypothesized that CaM binding to NOS-II is irreversible and independent of any changes in free [Ca^{2+}]. This implicates a permanent interdomain electron transfer between the oxygenase and reductase domain. Binding affinities and kinetics of CaM interaction with the CaM binding site are therefore critical for a complete understanding of the activation mechanism. It is also not known whether the high binding affinity of NOS-II for CaM is solely determined by the putative CaM-binding segment. Alternatively, one can predict a model where neighboring domains form a cave to trap CaM.

Putative CaM binding domains have been localized and characterized in various proteins, e.g. skeletal and smooth muscle myosin light-chain kinases, calcineurin, CaM kinase, and adenylyl cyclase. CaM binding domains are characterized by segments of 14−26 amino acid residues that differ significantly from each other yet have in common an amphiphilic character (O'Neil & DeGrado, 1990; James et al., 1995; Crivici & Ikura, 1995). The interaction between CaM and its CaM-binding domain has been investigated by NMR spectroscopy and X-ray crystallography (Roth et al., 1991; Ikura et al., 1992; Meador et al., 1993; Zhang & Vogel, 1994; Zhang et al., 1995). Binding affinities of CaM were mainly determined with [^{125}I]calmodulin, by fluorescence titration experiments or by peptide competition studies [e.g. Hubbard and Klee (1987), Dasgupta et al. (1989), Meyer et

† Supported by grants from the Deutsche Forschungsgemeinschaft (Ko948/3-3 and Ko948/4-2).

* Corresponding author: K.-W. Koch, Institut für Biologische Informationsverarbeitung, Forschungszentrum Jülich, D-52425 Jülich, Germany. Telephone: 02461-613255. Fax: 02461-614216.

‡ Forschungszentrum Jülich.

§ Forschungsinstitut für Molekulare Pharmakologie.

⊗ Abstract published in *Advance ACS Abstracts,* June 1, 1996.

[1] Abbreviations: NO, nitric oxide; NOS, nitric oxide synthase; NOS-I, neuronal nitric oxide synthase type I; NOS-II, macrophage nitric oxide synthase type II; CaM, calmodulin; SPR, surface plasmon resonance; NHS, *N*-hydroxysuccinimide; EDC, *N*-ethyl-*N*′-[(dimethylamino)propyl]carbodiimide; PDEA, 2-(2-pyridinyldithio)ethaneamine hydrochloride; RU, resonance units; HPLC, high-performance liquid chromatography; SNP, sodium nitroprusside; k_a, association rate constant; k_d, dissociation rate constant; K_D, dissociation constant; GC, guanylyl cyclase.

S0006-2960(96)00445-X CCC: $12.00

al. (1992), Vorherr et al. (1993), Zhang and Vogel (1994), and Craescu et al. (1995)].

The aim of this study was to measure the dynamics for the binding of CaM to the putative CaM-binding domains of NOS-I and NOS-II using the surface plasmon resonance (SPR) spectroscopy (Jönsson et al., 1991; O'Shannassy et al., 1994; Szabo et al., 1995). We tested the hypothesis whether the apparently irreversible binding of CaM to NOS-II is solely controlled by the CaM-binding domain. We determined the dissociation constants for CaM bound to peptides that represent the CaM-binding domains of both NOS forms.

MATERIALS AND METHODS

Materials. HPLC grade acetonitrile was obtained from J. T. Baker (Phillipsburg, U.S.A.). Water was purified with a Mili-Q system (Millipore, Eschborn, Germany). Eluents were degassed by continous sparging with helium. All reagents were at least analytical reagent grade. Trifluoroacetic acid (TFA), phenol, and piperidine were supplied by Merck (Darmstadt, Germany). The Fmoc amino acids and 2-(1*H*-benzotriazol-1-yl)-1,1,3,3-tetramethyluronium tetrafluoroborate used in synthesis were obtained from Novabiochem (Bad Soden, Germany). Dimethylformamide and diisopropylethylamine were obtained from Fluka (Buchs, Switzerland). Triisopropylsilane and sinapinic acid were supplied by Aldrich (Steinheim, Germany). TentaGel S RAM resin was obtained from Rapp Polymere (Tübingen, Germany). Bovine brain calmodulin was from Sigma.

Peptide Synthesis, Purification, and Characterization. Peptides were synthesized automatically on a MilliGen 9050 peptide synthesizer by the solid-phase method using standard Fmoc chemistry in the continous flow mode. Synthesis was carried out on a 4-[[(2′,4′-dimethoxyphenyl)amino]methyl]-phenoxyacetamido resin (0.22 mmol/g) using Nα-Fmoc-protected amino acid derivatives (0.3 M) and 2-(1*H*-benzotriazol-1-yl)-1,1,3,3-tetramethyluronium tetrafluoroborate (0.3 M) as coupling reagent in the presence of 2 equiv of diisopropylethylamine in dimethylformamide (DMF). Single couplings were allowed to proceed for 20 min, N-terminal deblocking was carried out with 25% piperidine in DMF for 10 min, and all washes were made with DMF. Final cleavage from the resin and deprotection of side chain functionalities was achieved by a mixture of 88% TFA/5% phenol/5% H_2O/2% triisopropylsilane for 3 h. Purification of 100 mg samples was carried out by preparative HPLC on PolyEncap A300 (10 μm, 250 × 20 mm inside diameter) (Bischoff Analysentechnik GmbH, Leonberg), using an acetonitrile/water−0.1% TFA solvent system (linear gradient of 25 to 45% acetonitrile in 70 min), to give final products >95% pure by HPLC analysis. HPLC analyses were carried out on a Shimadzu LC-10A gradient HPLC system consisting of two LC-10AD pumps, a SIL-10A autoinjector, a SPD-M10A diode array detector operating at 220 nm, and a CLASS-LC10 software package. Runs were carried out on a PolyEncap A300 column (250 × 4.6 mm inside diameter, 5 μm, Bischoff Analysentechnik GmbH, Leonberg): mobile phase A, 0.1% TFA in water; and B, 0.1% TFA in 50% acetonitrile/50% water (v/v), with a linear gradient of 20 to 80% B in 40 min. Peptides were characterized by matrix-assisted laser desorption/ionization mass spectrometry which gave the expected $[M + H]^+$ mass peaks on a linear time-of-flight mass spectrometer MALDI II (Kratos, Manchester) using the positive detection mode and a sinapinic acid matrix. In addition, amino acid analyses of purified peptides gave results which were consistent with the expected structures (hydrolysis in 6 N HCl at 110 °C for 22 h, Biotronik-Eppendorf LC 3000).

Immobilization of Peptides. Peptides corresponding to the putative CaM-binding domain of rat brain NOS-I and mouse macrophage NOS-II were immobilized to a Pharmacia sensor chip CM5 via the ligand thiol method. For this purpose, an additional cysteine was introduced at the NH_2-terminal part of the peptide. The carboxylated dextran matrix on the sensor chip surface was first activated by 10 μL of 50 mM *N*-hydroxysuccinimide (NHS) and 200 mM *N*-ethyl-*N*′-[(dimethylamino)propyl]carbodiimide (EDC) at a flow rate of 5 μL/min. The activated dextran matrix was modified by injection of 20 μL of 80 mM 2-(2-pyridinyldithio)-ethaneamine hydrochloride (PDEA) in 0.1 M sodium borate buffer (pH 8.5) at a flow rate of 5 μL/min. Ligands (peptides) were immobilized via thiol−disulfide exchange reaction by injection of 35 μL of NOS peptide (10 μg/mL) in 50 mM sodium formate buffer (pH 4.0). Reactive PDEA-modified dextran groups were deactivated by injection of 15 μL of 50 mM cysteine and 1 M NaCl.

Surface Plasmon Resonance Measurements. Biospecific interactions were monitored by surface plasmon resonance (SPR) using the BIAcore technology (Pharmacia). The kinetics of complex formation of CaM and the NOS peptides were studied by varying the concentration of CaM. CaM was dissolved at 6, 15, 30, 60, 150, 300, 450, 600, and 900 nM in 150 mM NaCl, 10 mM Hepes (pH 7.4), 3.4 mM EDTA, 5 mM $CaCl_2$, and 0.005% Tween-20 (running buffer). Afterward, 40 μL was injected into the flow cell at a flow rate of 5 μL/min. The binding and dissociation of CaM (the analyte) to the immobilized NOS peptide (the ligand) was monitored by a change in refractive index close to the surface of the thin gold film of the sensor chip CM5. Changes in the refractive index are directly correlated to changes in resonance units (RU) and recorded as sensorgrams. Dissociation of bound CaM was initiated by injecting running buffer without CaM. After each cycle, the sensor chip was regenerated by injection of 15 μL of running buffer without $CaCl_2$ in order to wash off any remaining CaM.

Analysis of Kinetic Data. Kinetic constants were obtained from sensorgrams according to the BIAcore theory (O'Shannessy et al.,1994; Szabo et al., 1995). The equation $dRU/dt = k_a[CaM]RU_{max} - (k_a[CaM] + k_d)RU_t$ allows the determination of rate constants from a plot of dRU/dt versus RU_t. The slope $k_a[CaM] + k_d$ of this plot is defined as k_s. Therefore, plotting k_s versus different [CaM] values allows the determination of the association and dissociation rate constants k_a and k_d, respectively. Alternatively, sensorgrams were analyzed by a nonlinear curve-fitting program using BIAevaluation software 2.1.

NOS Assay. As a source for neuronal NOS-I, we used a preparation of photoreceptor outer segments attached to parts of the inner segment (OS−IS) wherein NOS and soluble GC activities are present. NOS activity was monitored by the activation of a soluble GC via endogenously produced NO exactly as described (Koch et al., 1994; Zoche & Koch, 1995). Increasing amounts (10^{-9} to 10^{-6} M) of NOS-I peptide were used to bind endogenous present CaM and thus

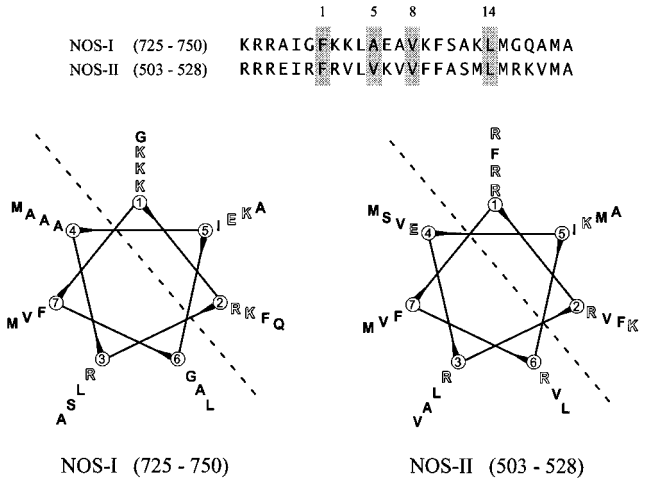

FIGURE 1: (upper part) Sequence alignment of peptides derived from NOS-I and NOS-II. The synthesized peptides of the hypothetical CaM binding sites correspond to residues 725−750 of rat brain NOS-I (Bredt et al., 1991) and to residues 503−528 of mouse macrophage NOS-II (Xie et al., 1992). Identical or conserved hydrophobic residues are in gray boxes. (lower part) Helical wheel projection of the peptides shown above. Charged residues are shown as open letters. The amphiphilic nature of these peptides is highlighted by the dashed lines.

to prevent NO synthesis. Increasing amounts of CaM (10^{-9} to 10^{-5} M) were added to reverse the inhibitory effect.

RESULTS

Peptides representing the putative CaM-binding domain of rat brain NOS-I and mouse macrophage NOS-II possess an amphiphilic character as illustrated in a helical wheel projection (Figure 1). In the NOS-I peptide, hydrophobic and charged residues are separated, a characteristic feature of a typical CaM-binding site. The amphiphilic character of the NOS-II peptide is less obvious. Biospecific interaction of the NOS-I peptide with CaM was demonstrated by an inhibitory effect on NOS-I activity from bovine retinae. If we incubate a preparation of bovine OS−IS with L-arginine and NADPH at micromolar free Ca^{2+}, we observed synthesis of NO sufficient to stimulate cGMP production by a soluble GC present in the same preparation (Koch et al., 1994; Zoche & Koch, 1995). Titration with the NOS-I peptides efficiently suppressed the soluble GC activity with an IC_{50} of 1.7×10^{-7} M (Figure 2A, open squares). The same NOS-I peptide harboring a biotin group instead of a cysteine at the NH_2 terminus gave a similar inhibition (Figure 2A, open circles). The peptides had no effect on cGMP production, when soluble GC was activated by SNP (filled symbols in Figure 2A). Inhibition by peptides was completely removed by the addition of CaM with an EC_{50} of 2.3×10^{-7} M (Figure 2B). The inhibitory effect of the same NOS-II peptide used in our SPR measurements was recently described on a preparation of macrophage NOS-II by Stevens-Truss and Marletta (1995).

Successful immobilization of peptides was achieved by thiol−disulfide exchange reaction. Figure 3 shows the immobilization of the NOS-I peptide on the sensor chip. Changes in resonance units (RU) correspond to changes in bulk refractive index during the steps of activation, immobilization, and deactivation. The amount of immobilized peptide was detectable at the end of the coupling procedure as a change in resonance units (ΔRU). We observed between

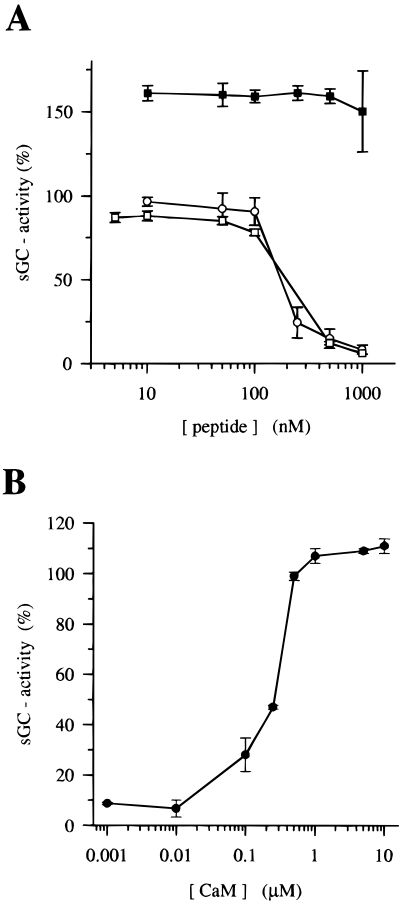

FIGURE 2: (A) Photoreceptor NOS activity was monitored by endogenous soluble GC (sGC) activity. Inhibition of NOS activity (open symbols) was achieved with increasing peptide concentrations: (○) NOS-I peptide with additional N-terminal Cys, $IC_{50} = 1.7 \times 10^{-7}$ M; (□) NOS-I peptide attached to biotin, $IC_{50} = 2.3 \times 10^{-7}$ M; and (■) control, direct stimulation of soluble GC with SNP. Addition of peptides was without effect. (B) Inhibition of NOS by peptides is CaM specific. Increasing [CaM] relieved inhibition by competitive binding to the peptide with an EC_{50} of 2.3×10^{-7} M. All measurements were done in triplicate (± SD).

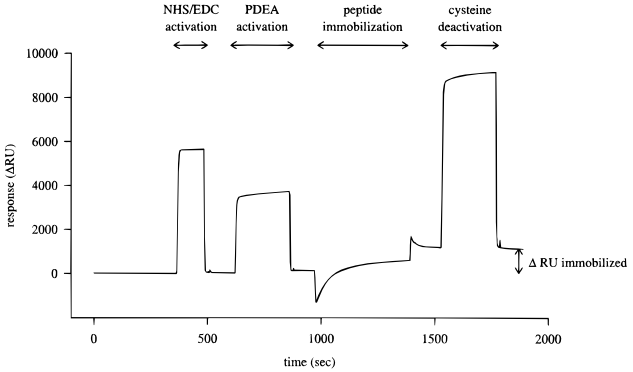

FIGURE 3: Sensorgram obtained during the immobilization of the NOS-I peptide. The carboxylated dextran was first activated by NHS/EDC and then modified by PDEA in order to allow a thiol disulfide exchange reaction with the free cysteine on the peptide. After binding of the peptide, excess reactive groups were deactivated by a pulse of cysteine. Covalent attachment of the peptide on the dextran layer resulted in a permanent change of resonance units (ΔRU) of 1249.

1121 and 2132 RU in five independent immobilization experiments. This corresponds to 1.1−2.1 ng/mm^2 immobilized peptide assuming that 1000 RU = 1 ng/mm^2, which is valid for most proteins and peptides.

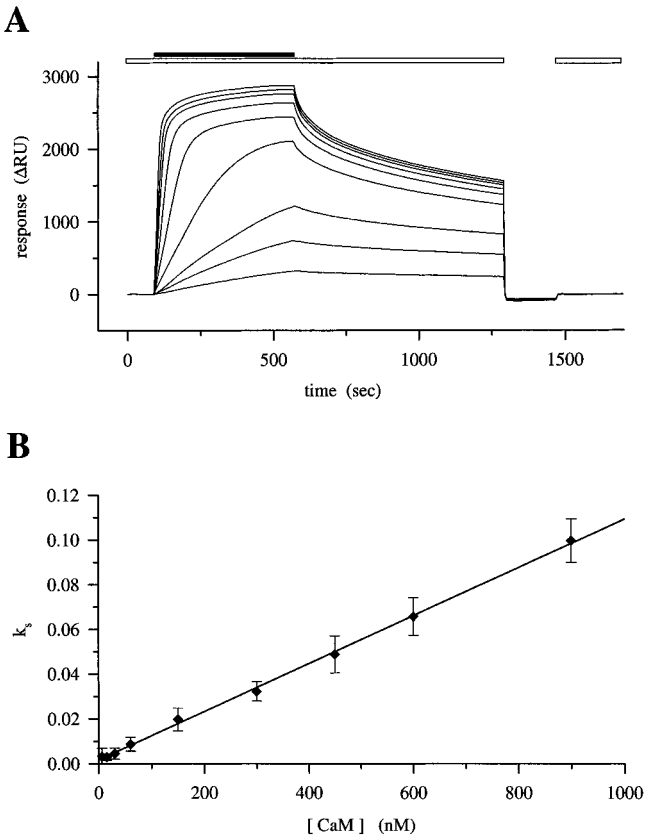

FIGURE 4: (A) Real time interaction analysis of CaM binding to immobilized NOS-I peptide. Sensorgrams were recorded using increasing amounts of CaM (6, 15, 30, 60, 150, 300, 450, 600, and 900 nM) in the running buffer during the association phase. Dissociation of the CaM peptide complex was initiated by omitting CaM in the buffer. Horizontal open bars represent flow of running buffer with Ca^{2+}; horizontal filled bars represent the presence of CaM in the running buffer. The regeneration pulse was delivered by the injection of buffer without Ca^{2+} and CaM (no bar). (B) Kinetic analysis of the data in panel A. For each sensorgram, a secondary plot of dRU/dt versus RU_t was constructed (not shown). The slope of this plot, k_s, was determined and plotted against different [CaM] values. k_s is defined as k_a[CaM] + k_d. Evaluating eight sets of sensorgrams as shown in panel A revealed the slope shown in panel B with $k_a = 1.1 \times 10^5$ M^{-1} s^{-1} and $k_d = 2.3 \times 10^{-3}$ s^{-1}.

Binding of CaM to the NOS-I peptide saturated at concentrations above 450 nM CaM. Maximal responses resulted in a ΔRU of 2700 or 2.7 ng/mm^2. Thus, 0.17 pmol/mm^2 CaM was bound to 0.26 pmol/mm^2 immobilized peptide at saturation, indicating that 65% of the immobilized peptide was accessible to CaM.

Sensorgrams at different [CaM] values were recorded at saturating [Ca^{2+}] to ensure optimal interaction of the Ca^{2+}-bound form of CaM with the peptide (Figure 4A). Sensorgrams consisted of three phases: an association phase, a dissociation phase, and a regeneration phase. Dissociation of the peptide−CaM complex during flushing of the flow cell with CaM-free buffer was followed by a decrease in resonance units. Complete dissociation was achieved by washing with EDTA (regeneration phase). The binding of CaM to the NOS-I peptide was Ca^{2+}-dependent; no binding was observed when excess EGTA or EDTA was present in the running buffer. Changes in refractive index caused by the running buffer without CaM gave very small rectangular step responses (ΔRU = 3−20 corresponding to 0.2−1.6% of signals at saturating [CaM]).

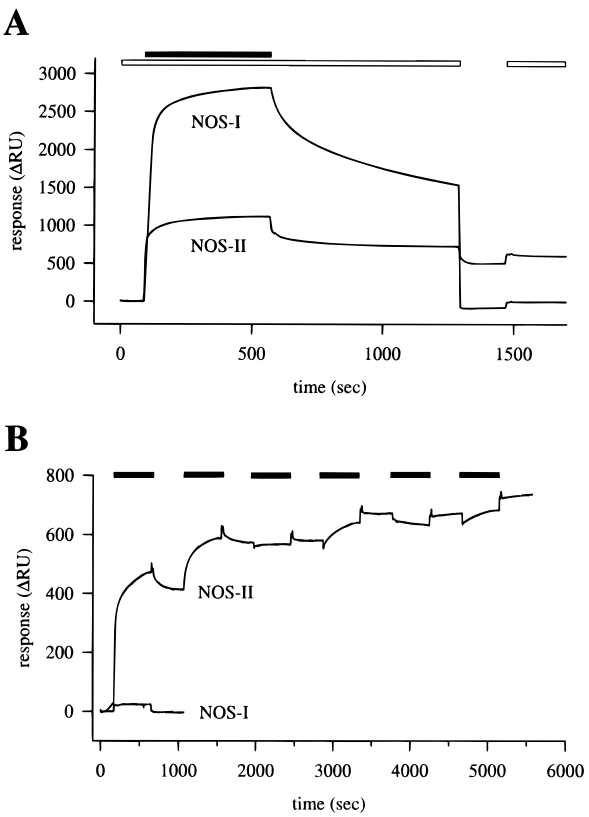

FIGURE 5: Comparison of CaM binding sites in NOS-I and NOS-II. (A) Sensorgrams were recorded with 600 nM CaM in the running buffer with excess Ca^{2+}. The dissociation signal was recorded by flushing the flow cell without CaM. (B) Complex formation of CaM and the NOS-II peptide in the absence of Ca^{2+}. Sensorgrams saturated after repetitive injections of CaM at ΔRU = 600. Only a small buffer signal was observed in the case of NOS-I peptide. Symbols have the same meaning as in Figure 4.

Sensorgrams in Figure 4A were analyzed by two different procedures. First, a derivative of the binding curve (or association phase), dRU/dt, was plotted as a function of the response RU_t, resulting in a linear relationship for each [CaM]. The slope of dRU/dt versus RU_t was used to construct a secondary plot k_s versus [CaM] (Figure 4B). We evaluated eight sets of measurements (an example of one set is given in Figure 4A). This yielded a straight line (Figure 4B) and allowed the determination of the association rate constant $k_a = 1.07$ (±0.12) × 10^5 M^{-1} s^{-1} from the slope and a dissociation rate constant $k_d = 1.82$ (±0.65) × 10^{-3} s^{-1} from the intercept with the ordinate. We calculated a dissociation constant $K_D = k_d/k_a = 1.7$ (±0.55) × 10^{-8} M. Alternatively, we determined the k_a and k_d values from the dissociation phase using a curve-fitting program. A simple association model A + B ↔ AB, where A is CaM and B is the immobilized peptide, was sufficient to fit the sensorgrams. By this procedure, we determined that $k_a = 1.58$ (±0.44) × 10^5 M^{-1} s^{-1} and for $k_d = 7.87$ (±0.64) × 10^{-4} s^{-1}, yielding a dissociation constant K_D of 5.0 (±0.83) × 10^{-9} M ($n = 72$). No significant change in kinetic constants was observed when the flow rate was varied (1, 2, 5, 10, 15, and 20 μL/min). Association and dissociation rate constants were not influenced by a variation in the amount of immobilized peptide.

Sensorgrams obtained with the macrophage NOS peptide were remarkably different (Figure 5). After complex formation, CaM did not dissociate again. The dissociation phase

obtained by flushing the cell with running buffer without CaM yielded almost a plateau (Figure 5A). The signal was unsuitable for evaluation by curve fitting. We can only give a rough estimation for the k_d of less than 10^{-6} s^{-1}. Fitting the association signal resulted in a k_a of 3×10^4 M^{-1} s^{-1}. The affinitiy is therefore in the subnanomolar range ($K_D < 1 \times 10^{-10}$ M). CaM, once bound to the peptide, was not removed by an EDTA regeneration pulse. Association of CaM to the NOS-II peptide also occurred in the absence of Ca^{2+} (3.4 mM EDTA in the running buffer; Figure 5B). Binding of CaM was saturated after repetitive injections to the same flow cell, and no further binding of CaM was achieved even with Ca^{2+} present. We detected no significant differences for the association and dissociation signal in the absence or presence of Ca^{2+}.

DISCUSSION

In this study, we have analyzed the interaction of CaM with peptides derived from NOS-I and NOS-II by SPR spectroscopy. The NOS-I peptide used in the SPR experiments showed an inhibitory effect in an enzyme competition experiment. The IC_{50} values differ from our K_D values by a factor of 10−20 since they were obtained by a complex assay system with coupled enzyme reactions. We performed this control experiment to show that the peptide is specific for CaM, i.e. that it can inhibit the Ca^{2+}/CaM-regulated NOS-I in solution. Addition of CaM could reverse the inhibitory effect (Figure 2B). Attachment of a large biotin group to the N-terminus did not change the inhibitory effect on NOS-I (Figure 2), showing that any modification at the N-terminus, i.e. the site of coupling to the dextran layer of the sensor chip, is without effect. Activation of the soluble GC by SNP was not influenced by the peptides, demonstrating that the locus of the peptide interaction is on CaM/NOS-I and not on the soluble GC.

Our determination of K_D values differs sligthly from previous reports that employ different techniques. Vorherr et al. (1993) measured a K_D of 1.8×10^{-9} M using fluorescence spectroscopy with dansyl-CaM. Zhang and Vogel (1994) derived a K_D of 2.2×10^{-9} M from peptide competition experiments with a CaM-regulated phosphodiesterase, and Schmidt et al. (1991) reported a $K_{0.5}$ for CaM of 3.5×10^{-9} M. We obtained a K_D of 5.0×10^{-9} M by curve fitting our sensorgrams which is in good agreement with these previous values. A significant difference was observed, if we estimated the K_D from a slope like in Figure 4B according to the BIAcore theory (O'Shannessy et al., 1994; Szabo et al., 1995). From there, we obtained a K_D of 1.7×10^{-8} M resulting mainly from a 2−3-fold lower dissociation rate constant. The association rate constants were almost identical for both evaluation methods. We are more confident with the data obtained by the curve-fitting procedure, since the graphical determination of k_d (intercept with the ordinate) resulted in larger errors (not shown).

Furthermore, we show that the two peptides exhibited a remarkable difference in the affinity for CaM. Whereas the NOS-I peptide reversibly bound CaM with nanomolar affinities, the binding of CaM to the NOS-II peptide was practically irreversible (Figure 5). These results show that the high affinity of CaM for NOS-II is only controlled by the CaM-binding domain and not by other parts of the molecule. Thus, CaM is trapped in NOS-II by binding to a small segment of 25 amino acids. Anagli et al. (1995) performed peptide displacement and fluorescence titration experiments with a similar peptide of a macrophage NOS-II and reported a K_D value of $<1 \times 10^{-9}$ M in the presence of Ca^{2+}. Compared to our estimation of K_D of $<1 \times 10^{-10}$ M (see above), there is a difference of about 1 order of magnitude, but errors inherent in our and their methods could account for the discrepancy.

Kinetic data obtained from SPR sensorgrams have the advantage of working with a label-free system. Changes in protein properties by introduction of for example a fluorescent label can be avoided by this approach, but SPR measurements have the disadvantage that the peptides or proteins must be immobilized. This could influence the binding kinetics or disturb the system. However, immobilization of proteins and peptides has long been successfully performed for many different purposes. In fact, many, if not most, proteins in the cytosol of a living cell are more or less restricted in their mobility, e.g. by an attachment to the cytoskeleton, filaments, membranes, or large protein complexes. This is even more true for protein modules like the CaM-binding site that is flanked by other domains.

SPR sensorgrams also allow us to discriminate between association and dissociation rate constants and to investigate stoichiometries during complex formation. Our kinetic data of CaM interacting with NOS-I and NOS-II might help us understand the different steps of NOS activation in more quantitative ways. Association of CaM to the NOS-I peptide was over 5-fold faster than that to the NOS-II peptide. Although the association rate constant was below the diffusion-controlled limit, a faster association (and dissociation) of CaM to NOS-I reflects the physiological necessity for a rapid switch on this Ca^{2+}-regulated enzyme.

At present, it is unclear which amino acids in a CaM-binding domain change a site of moderate binding affinity (like in NOS-I) into a site of very high binding affinity (like in NOS-II). Binding of CaM to NOS-I was strictly controlled by Ca^{2+}, in contrast to the Ca^{2+}-independent CaM−NOS-II interaction (Figures 4 and 5). Systematic amino acid substitutions in CaM-binding domains and subsequent analysis by SPR spectroscopy seem to be a valuable strategy to determine biologically significant changes in binding affinity.

ACKNOWLEDGMENT

We thank Mrs. D. Höppner-Heitmann for excellent technical assistance and Dr. U. B. Kaupp for critical comments on the manuscript.

REFERENCES

Abu-Soud, H. M., & Stuehr, D. J. (1993) *Proc. Natl. Acad. Sci. U.S.A. 90*, 10769−10772.

Anagli, J., Hofmann, F., Quadroni, M., Vorherr, T., & Carafoli, E. (1995) *Eur. J. Biochem. 233*, 701−708.

Bredt, D. S., & Snyder, S. H. (1994) *Annu. Rev. Biochem. 63*, 175−195.

Bredt, D. S., Hwang, P. M., Glatt, C. E., Lowenstein, C., Reed, R. R., & Snyder, S. H. (1991) *Nature 351*, 714−718.

Cho, H. J., Xie, Q.-W., Calaycay, J., Mumford, R. A., Swiderek, K. M., Lee, T. D., & Nathan, C. (1992) *J. Exp. Med. 176*, 599−604.

Craescu, C. T., Bouhss, A., Mispelter, J., Diesis, E., Popescu, A., Chiriac, M., & Bârzu, O. (1995) *J. Biol. Chem. 270*, 7088−7096.

Crivici, A., & Ikura, M. (1995) *Annu. Rev. Biophys. Biomol. Struct. 24*, 85−116.

Dasgupta, M., Honeycutt, T., & Blumenthal, D. K. (1989) *J. Biol. Chem. 264*, 17156−17163.
Griffith, O. W., & Stuehr, D. J. (1995) *Annu. Rev. Physiol. 57*, 707−736.
Hubbard, M. J., & Klee, C. B. (1987) *J. Biol. Chem. 262*, 15062−15070.
Ikura, M., Clore, G. M., Gronenborn, A. M., Zhu, G., Klee, C. B., & Bax, A. (1992) *Science 256*, 632−638.
James, P., Vorherr, T., & Carafoli, E. (1995) *Trends Biochem. Sci. 20*, 38−42.
Jannssens, S. P., Shimouchi, A., Quertermous, T., & Bloch, K. D. (1992) *J. Biol. Chem. 267*, 15274−15276.
Jönsson, U., Fägerstam, L., Ivarsson, B., Johnsson, B., Karlsson, R., Lundh, K., Löfås, S., Persson, B., Roos, H., Rönnberg, I., Sjölander, S., Sternberg, E., Ståhlberg, R., Urbaniczky, C., Östlin, H., & Malmqvist, M. (1991) *BioFeature 11*, 620−627.
Koch, K.-W., Lambrecht, H.-G., Haberecht, M., Redburn, D., & Schmidt, H. H. H. W. (1994) *EMBO J. 13*, 3312−3320.
Lamas, S., Marsden, P. A., Li, G. K., Tempst, P., & Michel, T. (1992) *Proc. Natl. Acad. Sci. U.S.A. 89*, 6348−6352.
Lowenstein, C. J., Glatt, C. S., Bredt, D. S., & Snyder, S. H. (1992) *Proc. Natl. Acad. Sci. U.S.A. 89*, 6711−6715.
Lyons, C. R., Orloff, G. J., & Cunningham, J. M. (1992) *J. Biol. Chem. 267*, 6370−6374.
Marletta, M. A. (1994) *Cell 78*, 927−930.
Meador, W. E., Means, A. R., & Quiocho, F. A. (1993) *Science 262*, 1718−1721.
Meyer, T., Hanson, P. I., Stryer, L., & Schulman, H. (1992) *Science 256*, 1199−1202.
Nathan, C., & Xie, Q.-W. (1994) *Cell 78*, 915−918.
O'Neil, K. T., & DeGrado, W. F. (1990) *Trends Biochem. Sci. 15*, 59−64.
O'Shannessy, D. J., Brigham-Burke, M., Soneson, K. K., Hensley, P., & Brooks, I. (1994) in *Methods in Enzymology*, Vol. 240, pp 323−349, Academic Press, New York.
Roth, S. M., Schneider, D. M., Strobel, L. A., VanBerkum, F. A., Means, A. R., & Wand, A. J. (1991) *Biochemistry 30*, 10078−10084.
Schmidt, H. H. H. W., & Walter, U. (1994) *Cell 78*, 919−925.
Schmidt, H. H. H. W., Pollock, J. S., Nakane, M., Gorsky, L. D., Förstermann, U., & Murad, F. (1991) *Proc. Natl. Acad. Sci. U.S.A. 88*, 365−369.
Schmidt, H. H. H. W., Smith, R. M., Nakane, M., & Murad, F. (1992) *Biochemistry 31*, 3243−3249.
Stevens-Truss, R., & Marletta, M. A. (1995) *Biochemistry 34*, 15638−15645.
Szabo, A., Stolz, L., & Granzow, R. (1995) *Curr. Opin. Struct. Biol. 5*, 699−705.
Vorherr, T., Knöpfel, L., Hofmann, F., Mollner, S., Pfeuffer, T., & Carafoli, E. (1993) *Biochemistry 32*, 6081−6088.
Xie, Q.-W., Cho, H. J., Calaycay, J., Mumford, R. A., Swiderek, K. M., Lee, T. D., Ding, A., Troso, T., & Nathan, C. (1992) *Science 256*, 225−228.
Zhang, M., & Vogel, H. J. (1994) *J. Biol. Chem. 269*, 981−985.
Zhang, M., Yuan, T., Aramini, J. M., & Vogel, H. J. (1995) *J. Biol. Chem. 270*, 20901−20907.
Zoche, M., & Koch, K.-W. (1995) *FEBS Lett. 357*, 178−182.

BI960445T